Supplementary Information

Solvent Effects of N, N-dimethylformamide and Methanol on Mass Spectrometry Imaging by Tapping-mode Scanning Probe Electrospray Ionization

Yoichi Otsuka[1,2,3], Nijiho Ote[4], Mengze Sun[1], Shuichi Shimma[5], Osamu Urakawa[6], Shinichi Yamaguchi[7], Tomoya Kudo[7], Michisato Toyoda[1,3]

[1]Department of Physics, Graduate School of Science, Osaka university
[2] JST PREST
[3] Forefront Research Center, Graduate School of Science, Osaka university
[4] Department of Biological Science, School of Science, Osaka university
[5] Department of Biotechnology, Graduate School of Engineering, Osaka university
[6] Department of Chemistry, Graduate School of Science, Osaka university
[7] Shimadzu Corporation

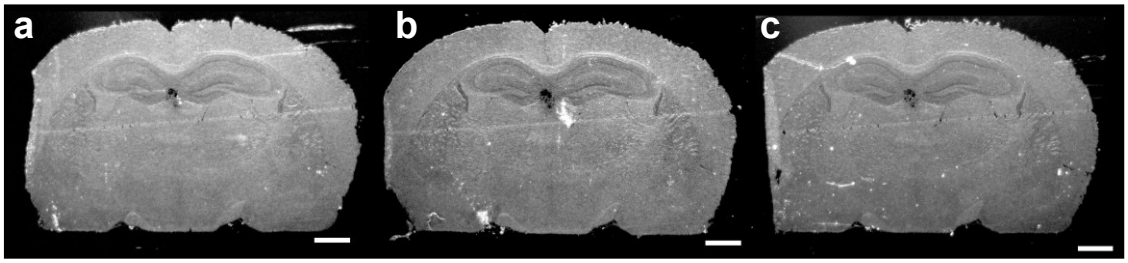

Fig. S1. Optical microscopy images of mouse brain tissue sections.

(a), (b) and (c) show mouse brain tissue sections prepared for MSI using DMF, the mixed solvent and MeOH, respectively. Scale bar = 1 mm.

Fig. S2. Results of MSI of mouse brain sections.

List of ion images in category 1

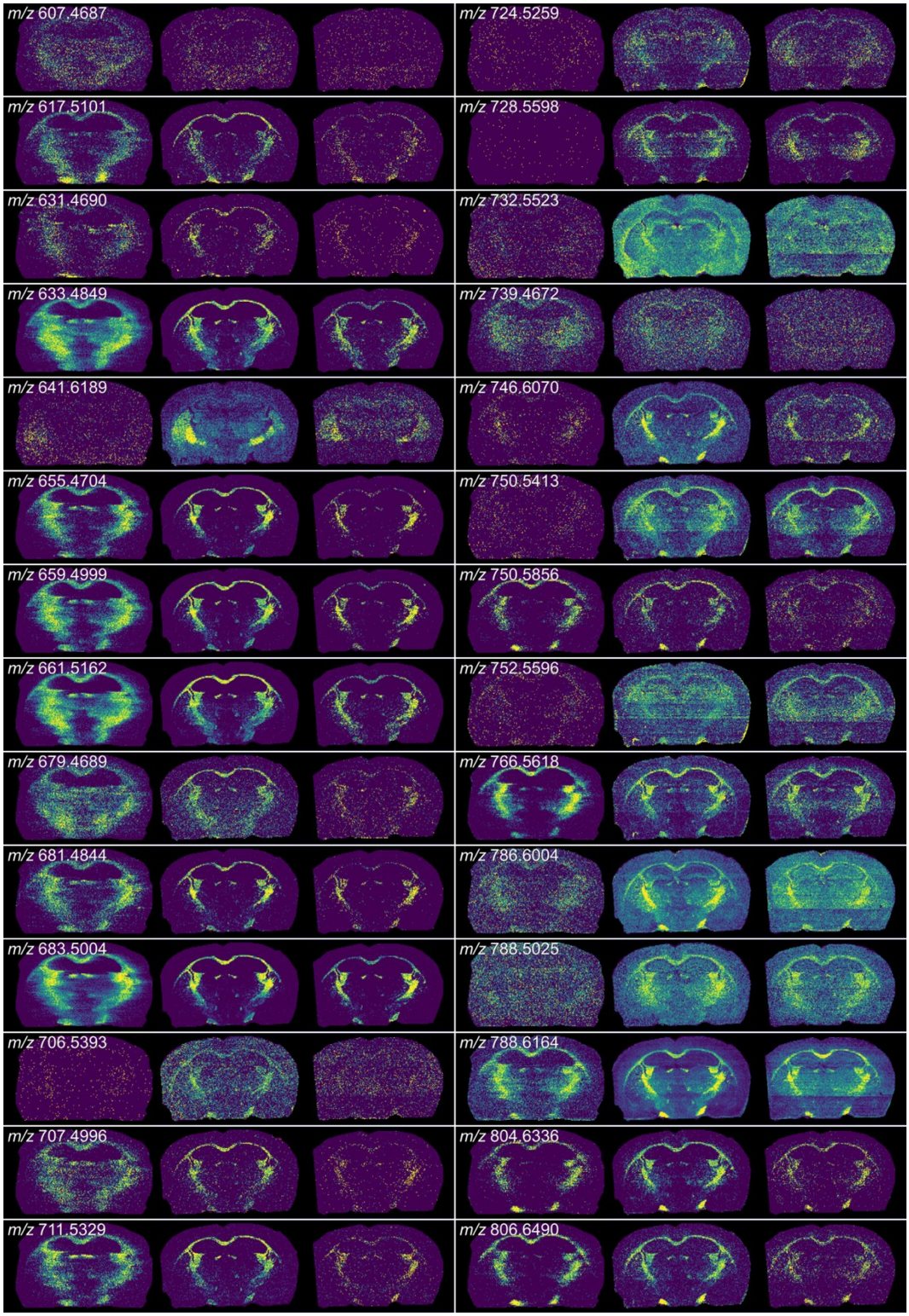

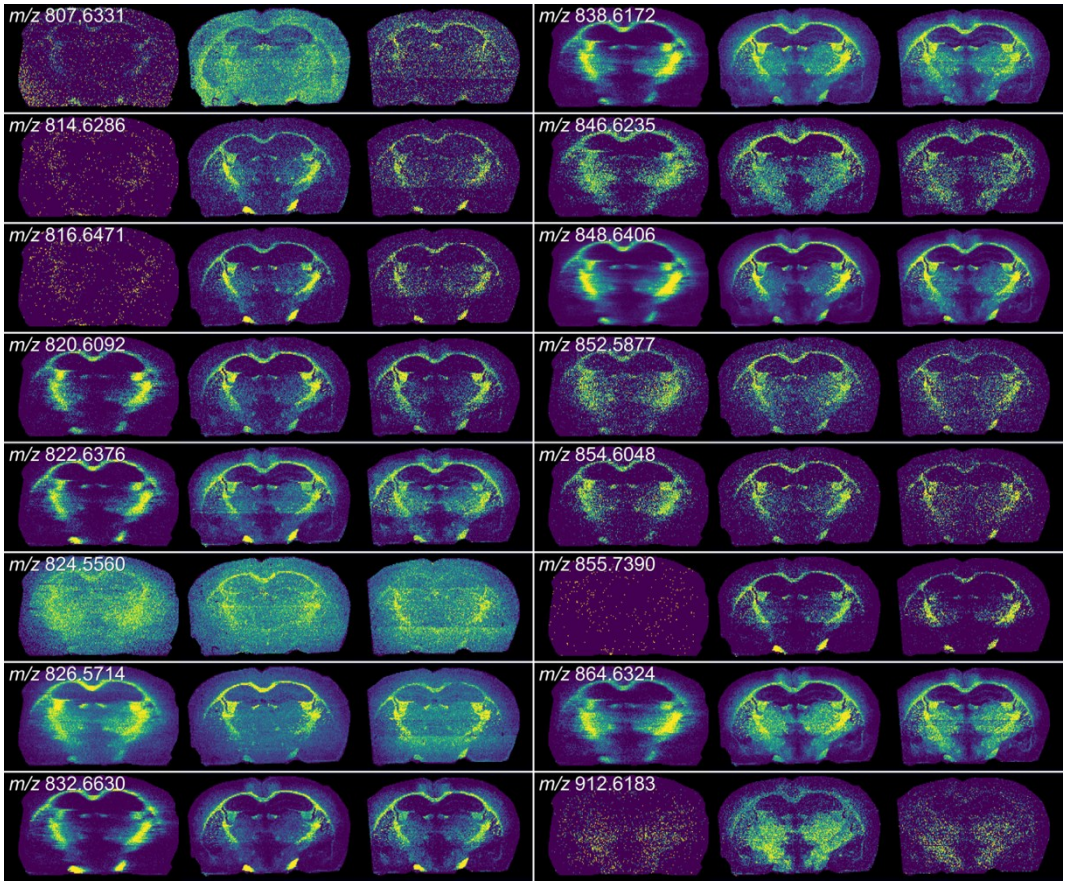
m/z 807.6331
m/z 838.6172
m/z 814.6286
m/z 846.6235
m/z 816.6471
m/z 848.6406
m/z 820.6092
m/z 852.5877
m/z 822.6376
m/z 854.6048
m/z 824.5560
m/z 855.7390
m/z 826.5714
m/z 864.6324
m/z 832.6630
m/z 912.6183

List of ion images in category 2

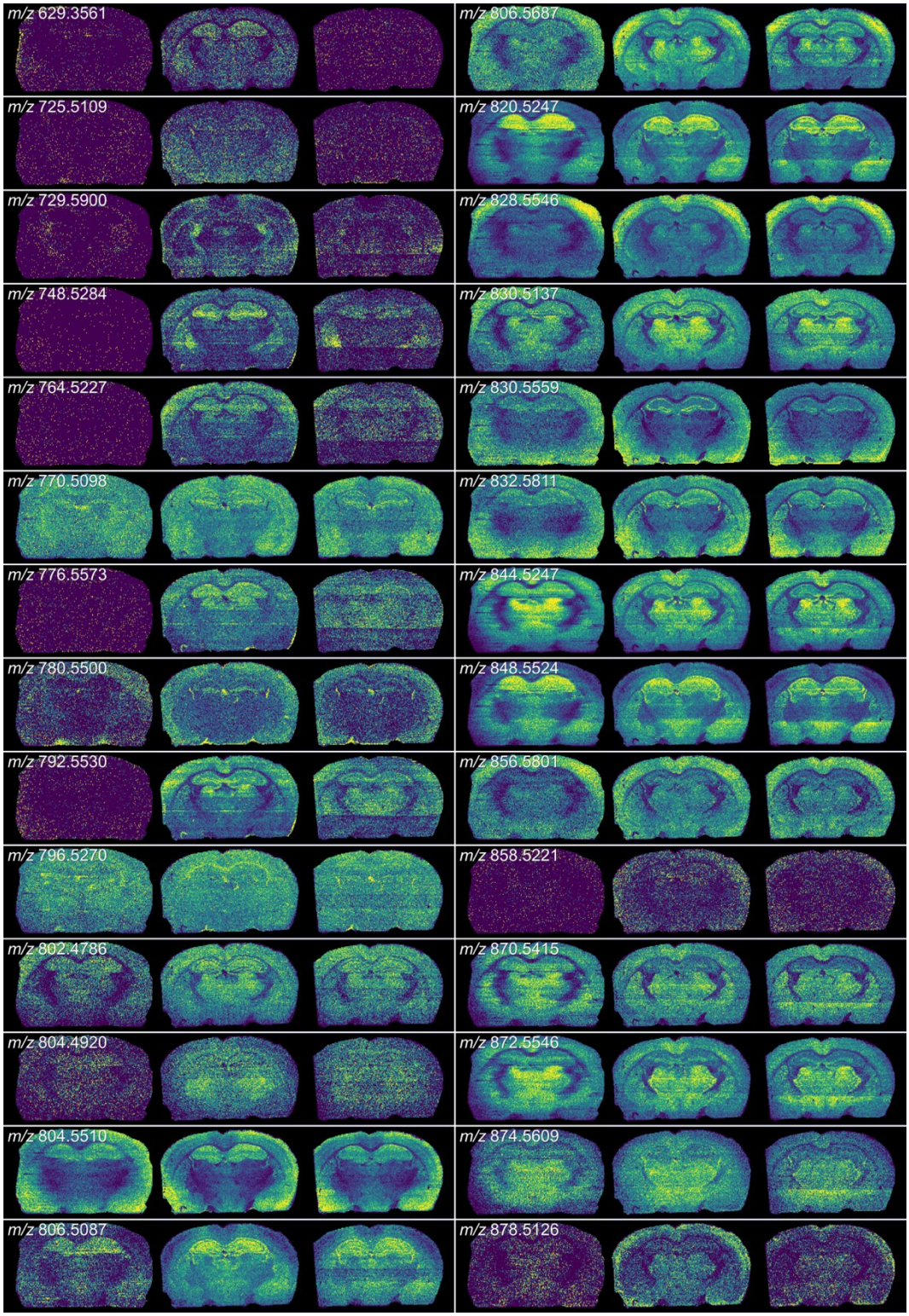

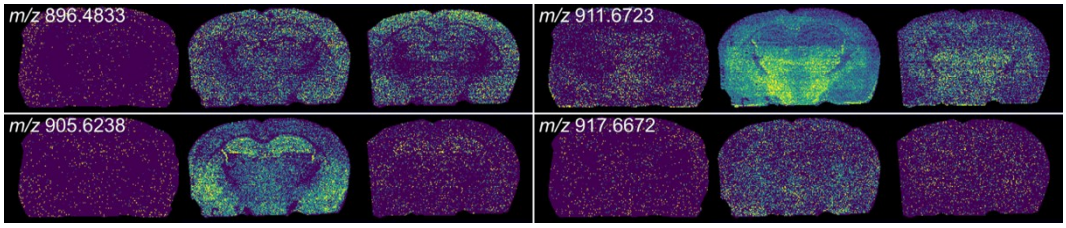

List of ion images in category 3

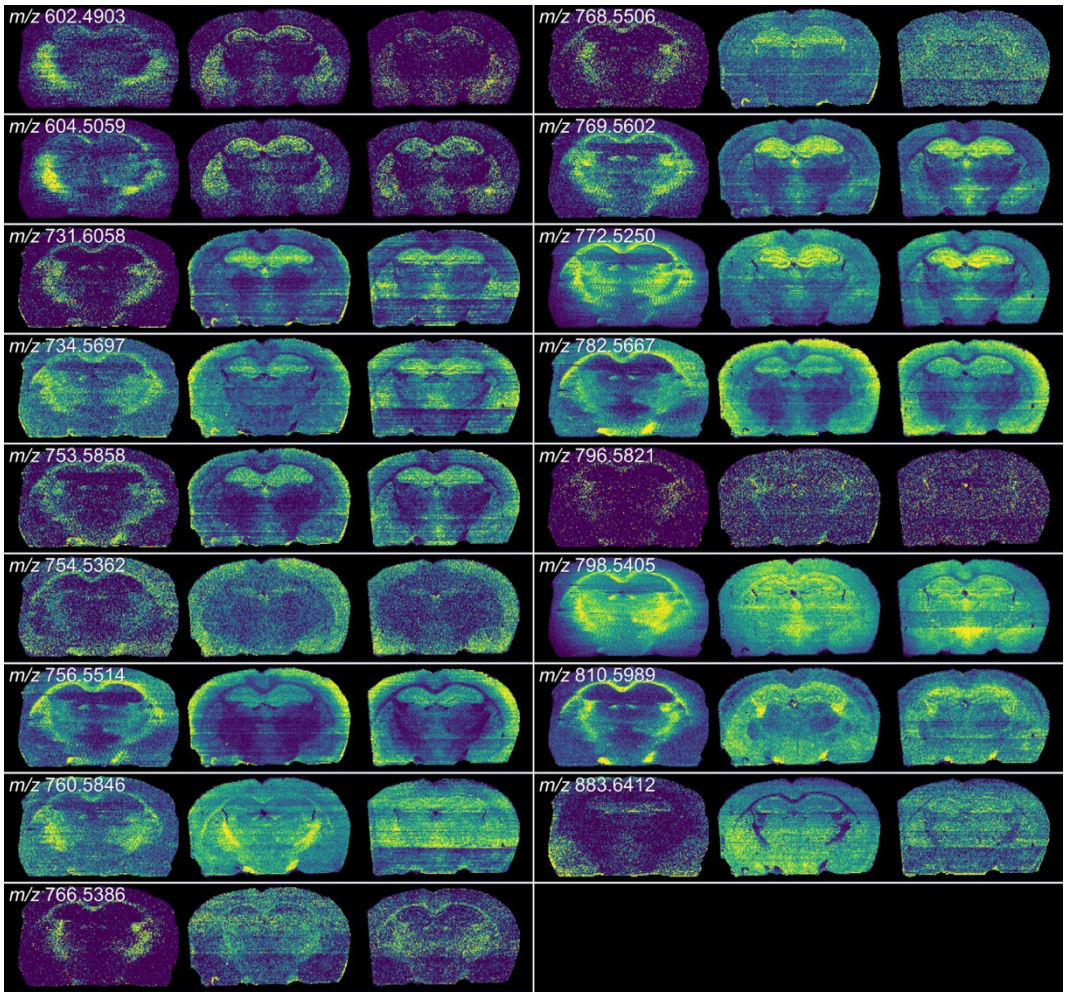

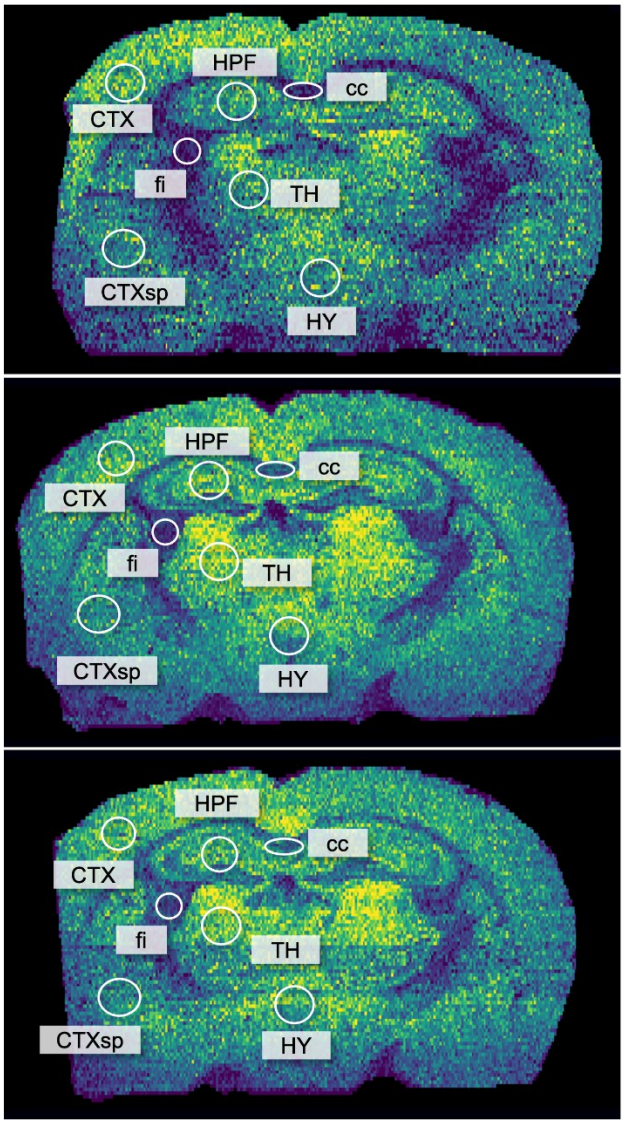

Fig. S3. The ROIs of mouse brain sections.

The ROIs are shown on the ion image at *m/z* = 830.5317 for (a) DMF, (b) the mixed solvent and (c) MeOH. fi: fimbria, cc: corpus callosum, TH: thalamus, HPF: hippocampal formation, HY: hypothalamus, CTX: cerebral cortex and CTXsp: cortical subplate

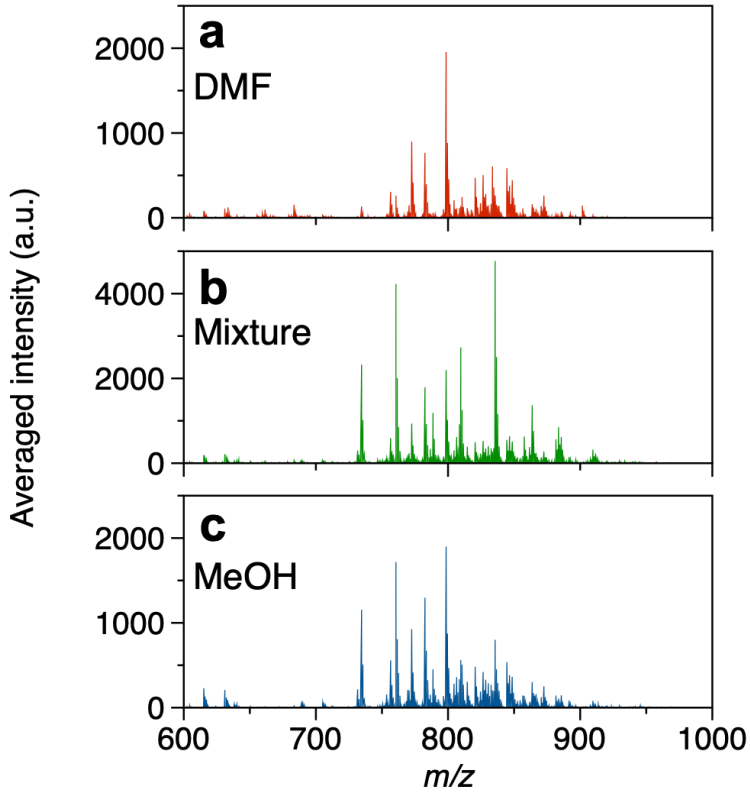

Fig. S4. Comparison of mass spectra of mouse brain sections.

(a), (b) and (c) show the average mass spectra of whole mouse brain tissue sections obtained in DMF, the mixed solvent and methanol, respectively.

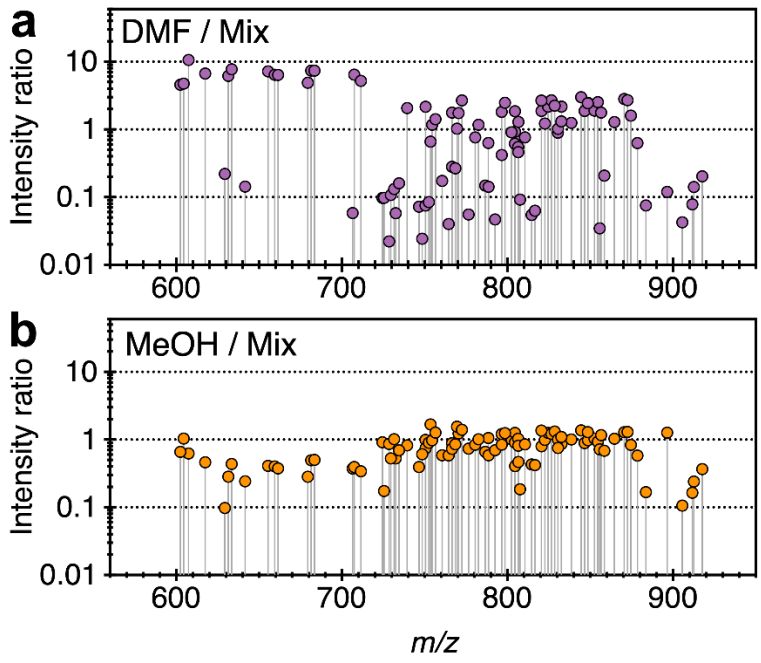

Fig. S5. Relationship between m/z and signal intensity ratio of ions.

Plots of signal intensity ratio of (a) DMF and (b) MeOH to the mixed solvent.

Fig. S6. Fiber tracts region in mouse brain sections.

The purple annotated regions correspond to the fiber tracts. Adapted from Allen Brain Atlas. (http://atlas.brain-map.org/atlas?atlas=1#atlas=1&plate=100960236&structure=1009&x=5291.2841796875&y=3387.2525024414062&zoom=-4&resolution=20.94&z=5)

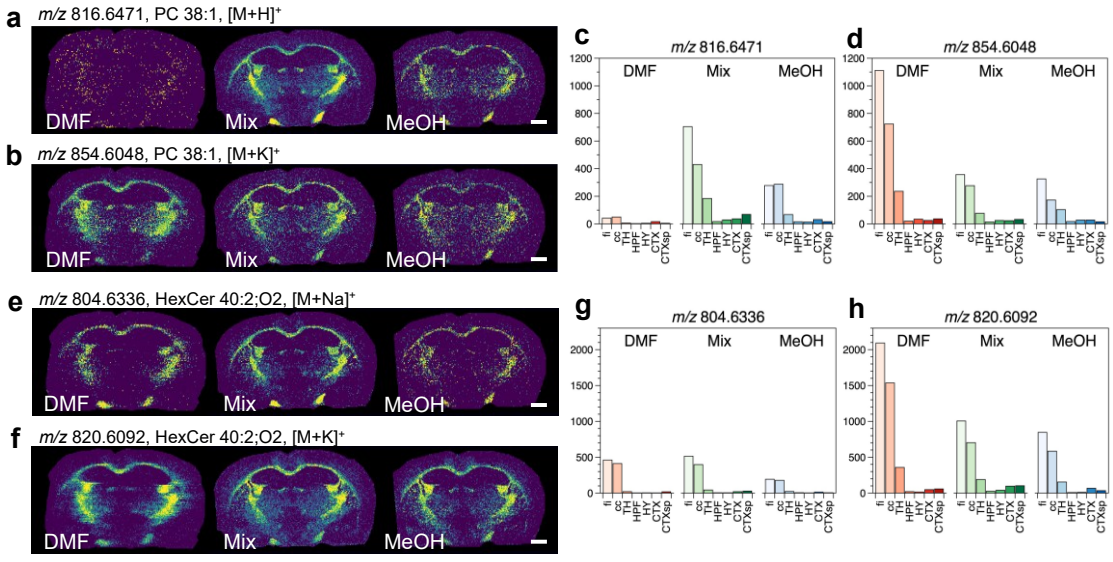

Fig. S7. Comparison of ion images obtained for mouse brain sections classified as Category 1.

Comparison of ion images obtained for mouse brain sections classified as Category 1, and the averaged signal intensities of the ROIs inside the brain. The *m/z* values of ions, assigned lipid species, and types of adduct ions are shown. Scale bar = 1 mm.

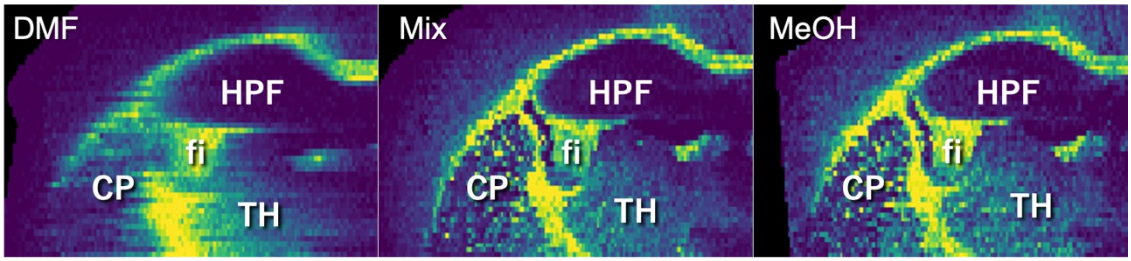

Fig. S8. Magnified images of lipid distributions in mouse brain sections.

Region names were added to Fig. 3(r) of the main manuscript. HPF: hippocampal formation, fi: fimbria, CP: caudoputamen and TH: thalamus.

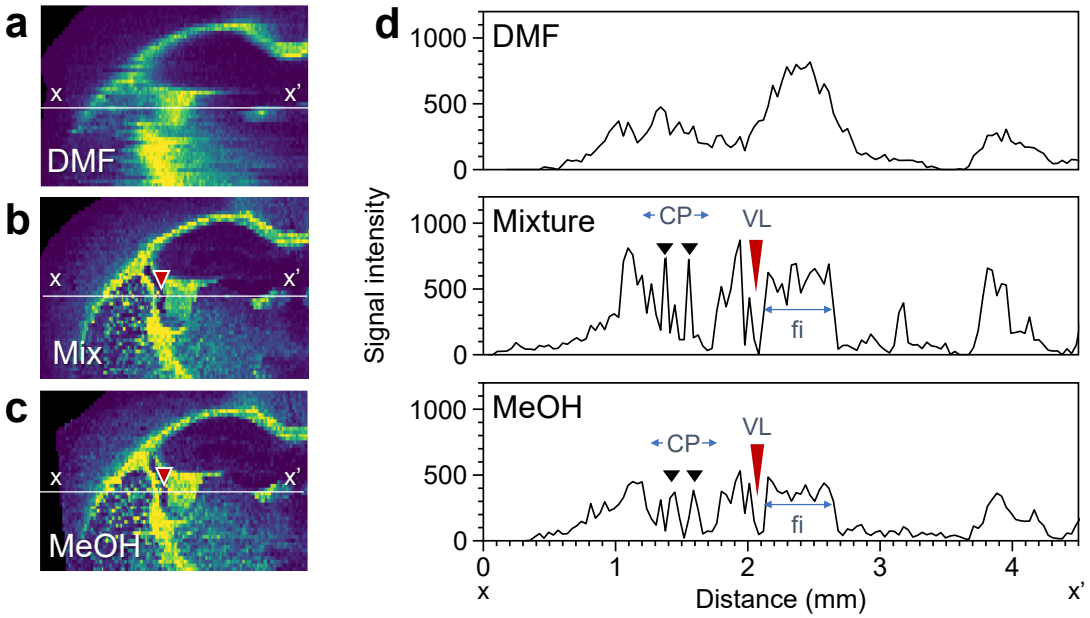

Fig. S9. Changes in spatial resolution of ion images with different solvents.

The ion images of *m/z* 848.6406 with (a) DMF, (b) Mixture and (c) MeOH. The signal intensity profiles corresponding to the white lines in the figures are shown in (d). With Mixture and MeOH, the signal difference between fimbria (fi) and adjacent lateral ventricle (VL) (red triangles) and the signal of localized lipids inside caudoputamen (CP) (black triangles) were obtained. On the other hand, it was difficult to visualize their spatial distribution when DMF was used.

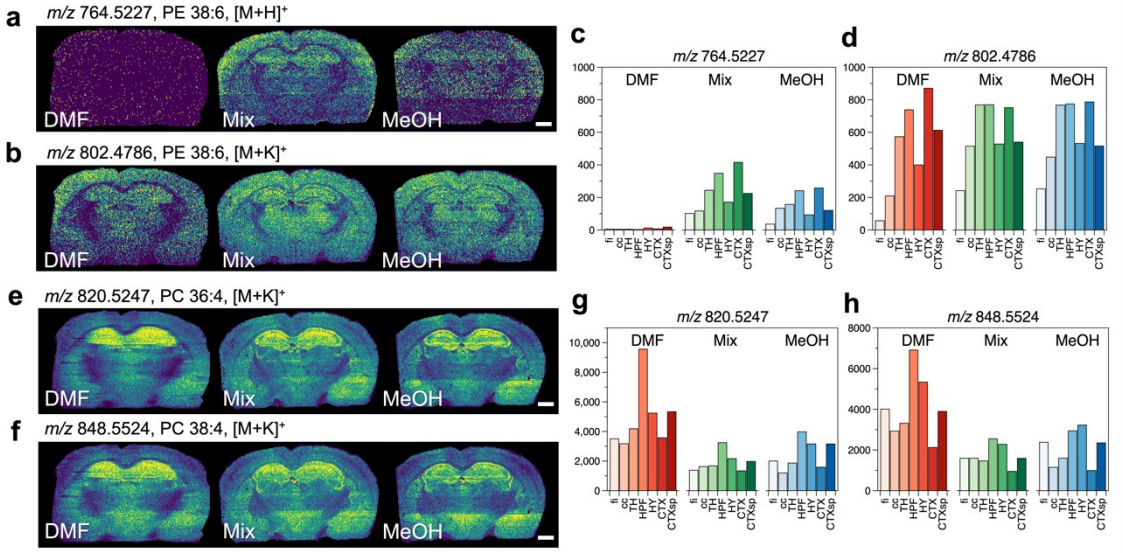

Fig. S10. Comparison of ion images obtained for mouse brain sections classified as Category 2. Comparison of ion images obtained for mouse brain sections classified as Category 1, and the averaged signal intensities of the ROIs inside the brain. The *m/z* values of ions, assigned lipid species, and types of adduct ions are shown. Scale bar = 1 mm.

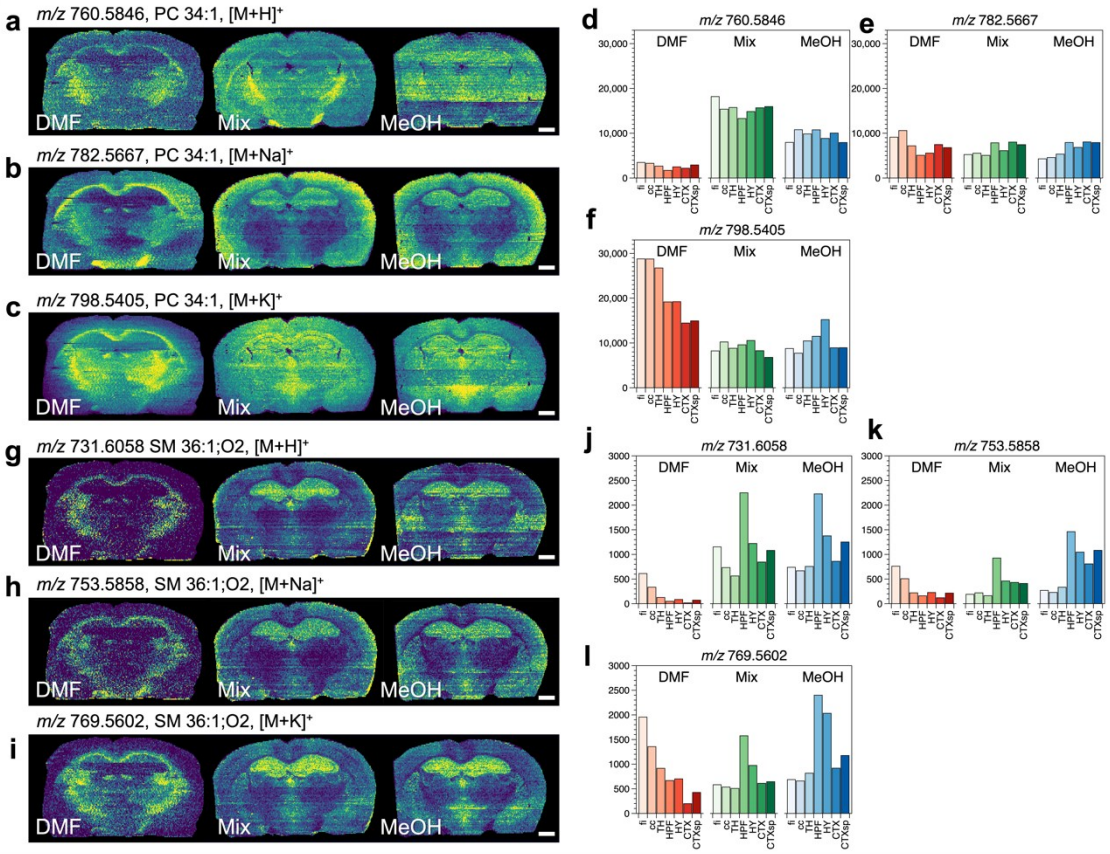

Fig. S11. Comparison of ion images obtained for mouse brain sections classified as Category 3. Comparison of ion images obtained for mouse brain sections classified as Category 3, and the averaged signal intensities of the ROIs inside the brain. The *m/z* values of ions, assigned lipid species, and types of adduct ions are shown. Scale bar = 1 mm.

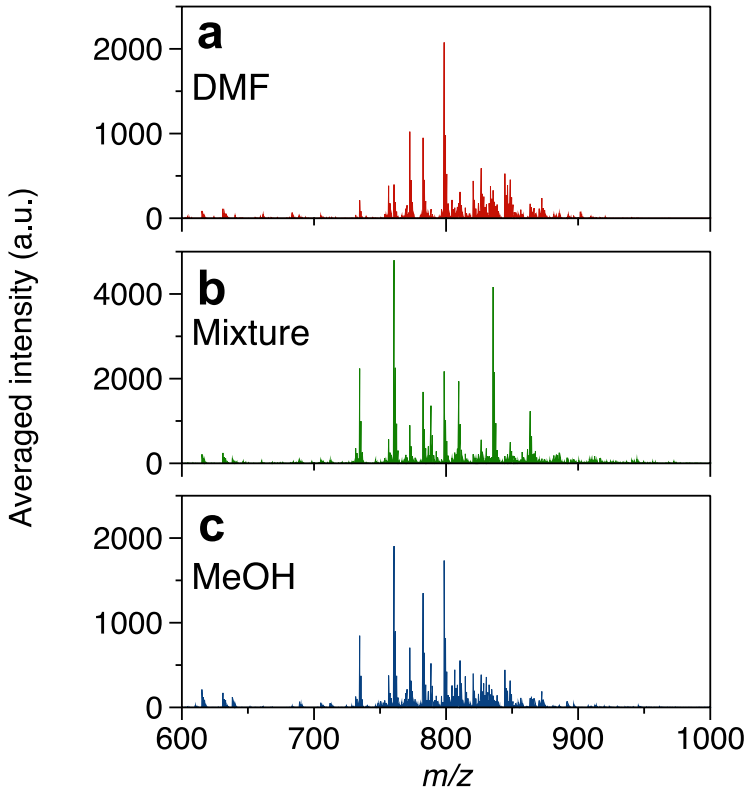

Fig. S12. Comparison of mass spectra of mouse brain sections.

(a), (b) and (c) show the average mass spectra of whole mouse brain tissue sections obtained in DMF, the mixed solvent and methanol, respectively. The different probes, brain sections and solvents from the measurements as shown in Fig. S4. were used.

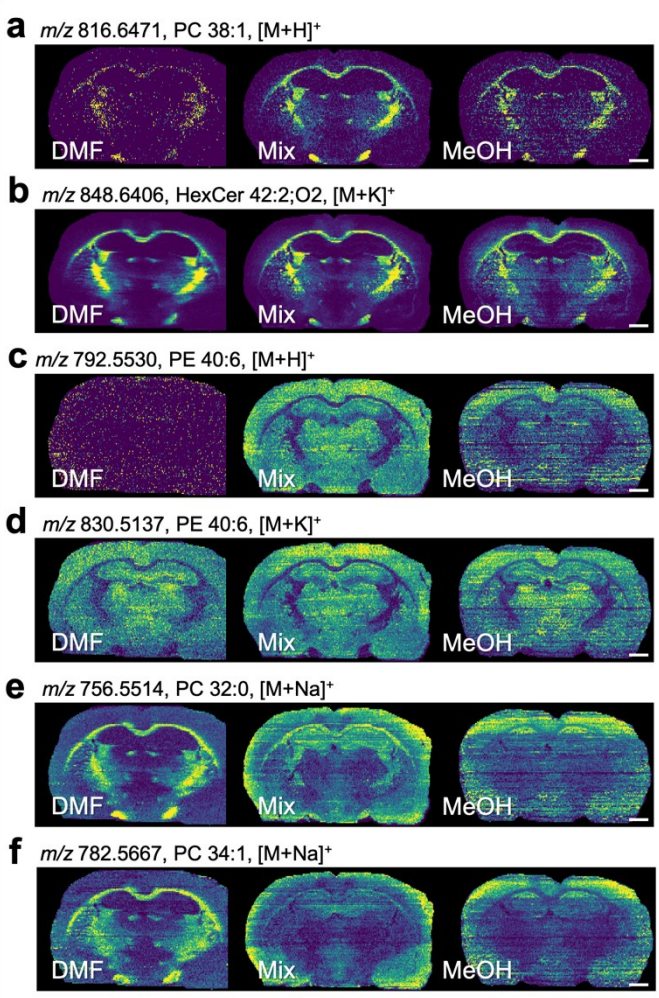

Fig. S13. Comparison of ion images for mouse brain sections for the check of reproducibility.

The *m/z* values of ions, assigned lipid species, and types of adduct ions are shown. Scale bar = 1 mm.

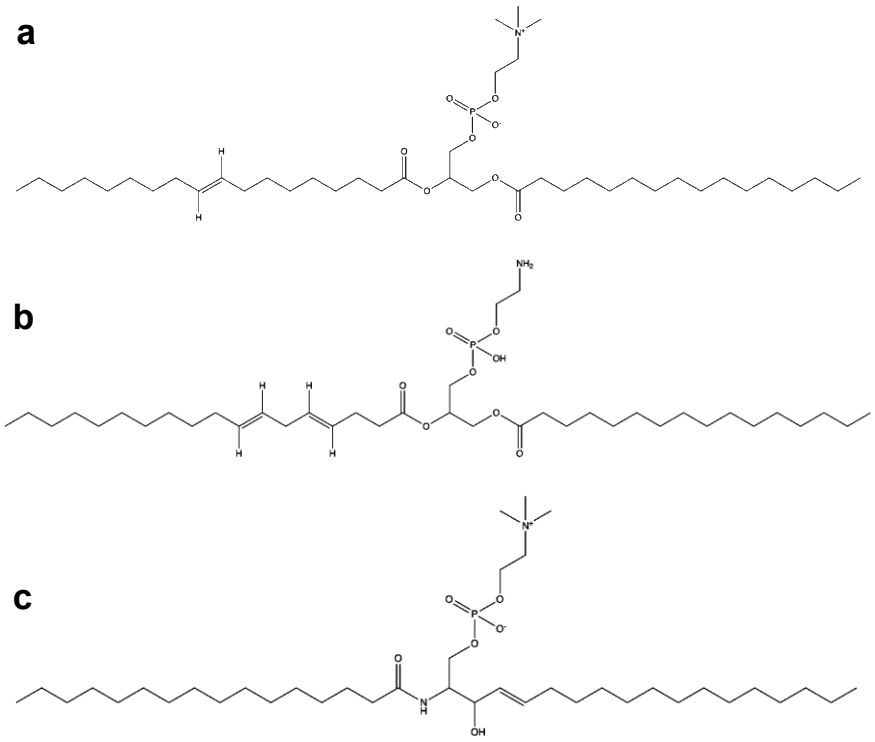

Fig. S14. Molecular structure of lipids used for the analysis with Hansen solubility parameters.
(a) PC 34:1 (16:0/18:1), (b) PE 34:2 (16:0/18:2) and (c) SM 34:1 (d18:1/16:0).

Table S1. Assignment results for lipids (used in Figs. 2, 3, 4, S7, S12, S13).

Category	Measured *m/z*	Matched *m/z*	Delta ppm	Name	Ion
1	804.6336	804.6324	1.5	HexCer 40:2;O2	$[M+Na]^+$
1	814.6286	814.6320	4.2	PC 38:2	$[M+H]^+$
1	816.6471	816.6477	0.7	PC 38:1	$[M+H]^+$
1	820.6092	820.6063	3.5	HexCer 40:2;O2	$[M+K]^+$
1	832.6630	832.6637	0.8	HexCer 42:2;O2	$[M+Na]^+$
1	848.6406	848.6376	3.5	HexCer 42:2;O2	$[M+K]^+$
1	852.5877	852.5879	0.2	PC 38:2	$[M+K]^+$
1	854.6048	854.6036	1.4	PC 38:1	$[M+K]^+$
2	764.5227	764.5225	0.3	PE 38:6	$[M+H]^+$
2	792.5530	792.5538	1.0	PE 40:6	$[M+H]^+$
2	802.4786	802.4784	0.2	PE 38:6	$[M+K]^+$
2	804.5510	804.5514	0.5	PC 36:4	$[M+Na]^+$
2	820.5247	820.5253	0.7	PC 36:4	$[M+K]^+$
2	830.5137	830.5097	4.8	PE 40:6	$[M+K]^+$
2	844.5247	844.5253	0.7	PC 38:6	$[M+K]^+$
2	856.5801	856.5827	3.0	PC 40:6	$[M+Na]^+$
3	731.6058	731.6061	0.4	SM 36:1;O2	$[M+H]^+$
3	734.5697	734.5694	0.4	PC 32:0	$[M+H]^+$
3	753.5858	753.5881	3.1	SM 36:1;O2	$[M+Na]^+$
3	756.5514	756.5514	0.0	PC 32:0	$[M+Na]^+$
3	760.5846	760.5851	0.7	PC 34:1	$[M+H]^+$
3	769.5602	769.5620	2.3	SM 36:1;O2	$[M+K]^+$
3	772.5250	772.5253	0.4	PC 32:0	$[M+K]^+$
3	782.5667	782.5670	0.4	PC 34:1	$[M+Na]^+$
3	798.5405	798.5410	0.6	PC 34:1	$[M+K]^+$

Table S2. Assignment results for lipids.

Category	Measured *m/z*	Matched *m/z*	Delta ppm	Name	Ion
1	607.4687	607.4697	1.6	PA O-30:0	$[M+H]^+$
1	607.4687	607.4698	1.8	DG 32:0	$[M+K]^+$
1	617.5101	617.5115	2.3	DG 34:1	$[M+Na]^+$
1	631.4690	631.4697	1.1	PA O-32:2	$[M+H]^+$
1	631.4690	631.4698	1.3	DG 34:2	$[M+K]^+$

1	633.4849	633.4854	0.8	PA O-32:1	$[M+H]^+$
1	633.4849	633.4855	0.9	DG 34:1	$[M+K]^+$
1	641.6189	641.6207	2.8	WE 42:1	$[M+Na]^+$
1	655.4704	655.4698	0.9	DG 36:4	$[M+K]^+$
1	655.4704	655.4697	1.1	PA O-34:4	$[M+H]^+$
1	655.4704	655.4673	4.7	PA O-32:1	$[M+Na]^+$
1	659.4999	659.5010	1.7	PA O-34:2	$[M+H]^+$
1	659.4999	659.5011	1.8	DG 36:2	$[M+K]^+$
1	661.5162	661.5167	0.8	PA O-34:1	$[M+H]^+$
1	661.5162	661.5168	0.9	DG 36:1	$[M+K]^+$
1	679.4689	679.4697	1.2	PA O-36:6	$[M+H]^+$
1	679.4689	679.4698	1.3	DG 38:6	$[M+K]^+$
1	679.4689	679.4673	2.4	PA O-34:3	$[M+Na]^+$
1	681.4844	681.4854	1.5	PA O-36:5	$[M+H]^+$
1	681.4844	681.4855	1.6	DG 38:5	$[M+K]^+$
1	681.4844	681.4830	2.1	PA O-34:2	$[M+Na]^+$
1	683.5004	683.5010	0.9	PA O-36:4	$[M+H]^+$
1	683.5004	683.5011	1.0	DG 38:4	$[M+K]^+$
1	683.5004	683.4986	2.6	PA O-34:1	$[M+Na]^+$
1	706.5393	706.5381	1.7	PC 30:0	$[M+H]^+$
1	707.4996	707.4986	1.4	PA O-36:3	$[M+Na]^+$
1	707.4996	707.5010	2.0	PA O-38:6	$[M+H]^+$
1	707.4996	707.5011	2.1	DG 40:6	$[M+K]^+$
1	711.5329	711.5324	0.7	DG 40:4	$[M+K]^+$
1	711.5329	711.5323	0.8	PA O-38:4	$[M+H]^+$
1	711.5329	711.5299	4.2	PA O-36:1	$[M+Na]^+$
1	724.5259	724.5252	1.0	PE O-34:2	$[M+Na]^+$
1	724.5259	724.5276	2.3	PE O-36:5	$[M+H]^+$
1	728.5598	728.5589	1.2	PE O-36:3	$[M+H]^+$
1	728.5598	728.5565	4.5	PE O-34:0	$[M+Na]^+$
1	732.5523	732.5538	2.0	PC 32:1	$[M+H]^+$
1	739.4672	739.4675	0.4	PA 36:2	$[M+K]^+$
1	746.6070	746.6058	1.6	PC O-34:1	$[M+H]^+$
1	750.5413	750.5408	0.7	PE O-36:3	$[M+Na]^+$
1	750.5413	750.5432	2.5	PE O-38:6	$[M+H]^+$

1	750.5856	750.5854	0.3	HexCer 36:1;O2	$[M+Na]^+$
1	752.5596	752.5589	0.9	PE O-38:5	$[M+H]^+$
1	752.5596	752.5565	4.1	PC O-33:2	$[M+Na]^+$
1	752.5596	752.5565	4.1	PE O-36:2	$[M+Na]^+$
1	760.5846	760.5851	0.7	PC 34:1	$[M+H]^+$
1	766.5618	766.5594	3.1	HexCer 36:1;O2	$[M+K]^+$
1	786.6004	786.6007	0.4	PC 36:2	$[M+H]^+$
1	788.5025	788.4991	4.3	PE O-38:6	$[M+K]^+$
1	788.6164	788.6164	0.0	PC 36:1	$[M+H]^+$
1	806.6490	806.6480	1.2	HexCer 40:1;O2	$[M+Na]^+$
1	807.6331	807.6350	2.4	SM 40:2;O2	$[M+Na]^+$
1	822.6376	822.6371	0.6	PC O-40:5	$[M+H]^+$
1	822.6376	822.6347	3.5	PC O-38:2	$[M+Na]^+$
1	824.5560	824.5566	0.7	PC 36:2	$[M+K]^+$
1	824.5560	824.5552	1.0	SHexCer 36:1;O3	$[M+H]^+$
1	826.5714	826.5721	0.8	PE O-42:7	$[M+Na]^+$
1	826.5714	826.5723	1.1	PC 36:1	$[M+K]^+$
1	838.6172	838.6169	0.4	HexCer 40:1;O3	$[M+K]^+$
1	846.6235	846.6219	1.9	PS 40:1	$[M+H]^+$
1	855.7390	855.7412	2.6	TG 50:1	$[M+Na]^+$
1	864.6324	864.6325	0.1	HexCer 36:1;O	$[M+K]^+$
1	864.6324	864.6325	0.1	HexCer 42:2;O3	$[M+K]^+$
1	912.6183	912.6205	2.4	SHexCer 42:2;O2	$[M+Na]^+$
2	629.3561	629.3579	2.9	PA 28:1	$[M+K]^+$
2	725.5109	725.5116	1.0	PA 38:4	$[M+H]^+$
2	725.5109	725.5092	2.3	PA 36:1	$[M+Na]^+$
2	729.5900	729.5905	0.7	SM 36:2;O2	$[M+H]^+$
2	748.5284	748.5276	1.1	PE O-38:7	$[M+H]^+$
2	748.5284	748.5252	4.3	PE O-36:4	$[M+Na]^+$
2	770.5098	770.5097	0.1	PC 32:1	$[M+K]^+$
2	770.5098	770.5095	0.4	PE O-38:7	$[M+Na]^+$
2	776.5573	776.5565	1.0	PE O-38:4	$[M+Na]^+$
2	776.5573	776.5589	2.1	PE O-40:7	$[M+H]^+$
2	780.5500	780.5514	1.8	PC 34:2	$[M+Na]^+$
2	780.5500	780.5538	4.9	PC 36:5	$[M+H]^+$

2	796.5270	796.5253	2.1	PC 34:2	$[M+K]^+$
2	796.5270	796.5252	2.3	PE O-40:8	$[M+Na]^+$
2	796.5270	796.5239	3.9	SHexCer 34:1;O3	$[M+H]^+$
2	804.4920	804.4940	2.5	PE 38:5	$[M+K]^+$
2	804.4920	804.4940	2.5	PE O-38:6;O	$[M+K]^+$
2	806.5087	806.5097	1.2	PE 38:4	$[M+K]^+$
2	806.5087	806.5097	1.2	PE O-38:5;O	$[M+K]^+$
2	806.5687	806.5694	0.9	PC 38:6	$[M+H]^+$
2	806.5687	806.5670	2.1	PC 36:3	$[M+Na]^+$
2	828.5546	828.5538	1.0	PC 40:9	$[M+H]^+$
2	828.5546	828.5514	3.9	PC 38:6	$[M+Na]^+$
2	830.5559	830.5542	2	PC 36:4;O3	$[M+H]^+$
2	832.5811	832.5827	1.9	PC 38:4	$[M+Na]^+$
2	832.5811	832.5851	4.8	PC 40:7	$[M+H]^+$
2	848.5524	848.5566	4.9	PC 38:4	$[M+K]^+$
2	858.5221	858.5256	4.1	PS 40:6	$[M+Na]^+$
2	870.5415	870.5410	0.6	PC 40:7	$[M+K]^+$
2	872.5546	872.5566	2.3	PC 40:6	$[M+K]^+$
2	872.5546	872.5566	2.3	PE 43:6	$[M+K]^+$
2	874.5609	874.5652	4.9	Hex2Cer 32:0;O2	$[M+K]^+$
2	878.5126	878.5097	3.3	PE 44:10	$[M+K]^+$
2	896.4833	896.4838	0.6	PS 42:9	$[M+K]^+$
2	905.6238	905.6242	0.4	PG 44:4	$[M+Na]^+$
2	911.6723	911.6712	1.2	PG 44:1	$[M+Na]^+$
2	917.6672	917.6630	4.6	TG 56:12	$[M+Na]^+$
3	602.4903	602.4909	1.0	Cer 36:2;O2	$[M+K]^+$
3	604.5059	604.5065	1.0	Cer 36:1;O2	$[M+K]^+$
3	754.5362	754.5357	0.7	PC 32:1	$[M+Na]^+$
3	754.5362	754.5381	2.5	PC 34:4	$[M+H]^+$
3	766.5386	766.5381	0.7	PE 38:5	$[M+H]^+$
3	766.5386	766.5381	0.7	PE O-38:6;O	$[M+H]^+$
3	766.5386	766.5357	3.8	PE 36:2	$[M+Na]^+$
3	768.5506	768.5514	1.0	PE 36:1	$[M+Na]^+$
3	768.5506	768.5538	4.2	PE 38:4	$[M+H]^+$
3	768.5506	768.5538	4.2	PE O-38:5;O	$[M+H]^+$

3	796.5821	796.5827	0.8	PE 38:1	$[M+Na]^+$
3	796.5821	796.5851	3.8	PE 40:4	$[M+H]^+$
3	810.5989	810.5983	0.7	PC 36:1	$[M+Na]^+$
3	810.5989	810.6007	2.2	PC 38:4	$[M+H]^+$
3	883.6412	883.6423	1.2	PG 44:4	$[M+H]^+$
3	883.6412	883.6399	1.5	PG 42:1	$[M+Na]^+$

PC: phosphatidylcholines, PE: phosphatidylethanolamines, PA: phosphatidic acids, PS: phosphatidylserines, PG: phosphatidylglycerols, SM: sphingomyelins, DG: diacylglycerol, TG: triacylglycerol and HexCer: hexosylceramides.

Table S3. List of equipments used in t-SPESI system.

	Name	Model	Manufacturer
1	Probe vibration piezo actuator	PMF-3030	NTK ceratec, Japan
2	Probe piezo actuator HV amplifier	M-26110	Mess-tek, Japan
3	Photo diode	S5870	Hamamatsu photonics, Japan
4	Laser	TC20	Neoark, Japan
5	Band path filter	HMZ0660	Asahi optics, Japan
6	Laser controller	DPS-5004	Neoark, Japan
7	Lock-in amplifier	LI-5645	NF, Japan
8	Sample motor XY stage	OSMS(CS)2-035	Sigma, Japan
9	Sample motor XY stage controller	SHOT-302GS	Sigma, Japan
10	Sample motor Z stage	OSMS40-5ZF-0B	Sigma, Japan
11	Sample motor Z stage controller	SHOT-702	Sigma, Japan
12	Sample piezo Z stage	MTKK08S180F30	Mechano transformer, Japan
13	Sample piezo Z stage HV amplifier	M-26109	Mess-tek, Japan
14	Probe motor XY stage	HPS60-20X, HPS80-50X	Sigma, Japan
15	Probe motor XY stage controller	GSC-01	Sigma, Japan
16	Probe motor Z stage	OSMS20-85	Sigma, Japan
17	Probe motor Z stage controller	GSC-01	Sigma, Japan
18	Anti-vibration stage	HAX-0405	Nihon boshink kogyo, Japan
19	Inlet Heater controller	MTCS	Misumi, Japan
20	Inlet voltage supply	PMX500-0.1A	Kikusui, Japan
21	PC	Precision 3630 Tower	Dell, USA
22	Software	LabVIEW 2020	NI, USA
23	Compact RIO	cRIO-9047	NI, USA
24	Analog input module	NI 9215	NI, USA
25	Analog output module	NI 9263	NI, USA
26	Relay module	NI 9482	NI, USA
27	Syringe pump	Legato 185	KD scientific, USA
28	Diaphragm pump	DA-30D	ULVAC, Japan
29	Mass flow controller	3665-1/4SWL-AIR-36SLM-20℃	Kofloc, Japan

29	Mass spectrometer	LCMS-9030	Shimadzu, Japan
30	Precolumn Filter	A-355	Upchurch Scientific, USA

Table S4. Experimental condition for checking the reproducibility

Solvent	Flow rate (nL/min)	Probe oscillation Frequency (Hz)	Solvent voltage (kV)
MeOH	35	684.9	5
Mixed solvent	35	684.2	5
DMF	35	690.1	5

Table S5. Hansen solubility parameters of solvents[1,2].

	δ_D	δ_P	δ_H
MeOH	15.1	12.3	22.3
Mixed solvent	16.0	13.0	16.8
DMF	17.4	13.7	11.3

δ_D, δ_P, and δ_H correspond to the London dispersion force term, dipole-to-dipole force term, and hydrogen bonding force term in the Hansen solubility parameter, respectively.

Table S6. Hansen solubility parameters of lipids[3]

Lipids	δ_D	δ_P	δ_H	R_0
PC (16:0/18:1)	16.1	6.4	9.1	10
PE (16:0/18:2)	16.2	7.1	9.8	10
SM (d18:1/16:0)	16.1	9.6	11.4	10

Table S7. R_a of solvents with lipids

Ra	PC 34:1	PE 34:2	SM 34:1
MeOH	14.6	13.7	11.4
Mixed solvent	10.1	9.2	6.4
DMF	8.1	7.2	4.9

Section S1. Estimation of capillary number

Capillary number (Ca) is a dimensionless number expressed by the following equation.

$$Ca = U\mu/\gamma$$

Where, U, μ and γ are the stretching speed, viscosity, surface tension of the solvent, respectively. The values for μ and γ were estimated from experimental values. U was estimated with the following contents.

Estimation of stretching speed of liquid bridge

We used the time variation of the probe tip velocity which was determined from the resonant frequency and amplitude of the probe oscillation and the time to break the liquid bridge on the probe tip. The probe oscillates at the resonant frequency, and the displacement ($y(t)$), velocity ($v(t)$) and acceleration ($a(t)$) of the probe tip are given by the equations below.

$$y(t) = A\ \sin(\omega t)$$
$$v(t) = A\omega \cos(\omega t)$$
$$a(t) = -A\omega^2 \sin(\omega t)$$
$$\omega = 2\pi f$$

Fig. S15 shows the values of $y(t), v(t)$ and $a(t)$ for the probe which is oscillation at 700 Hz of resonant frequency with 0.5 mm of oscillation amplitude.

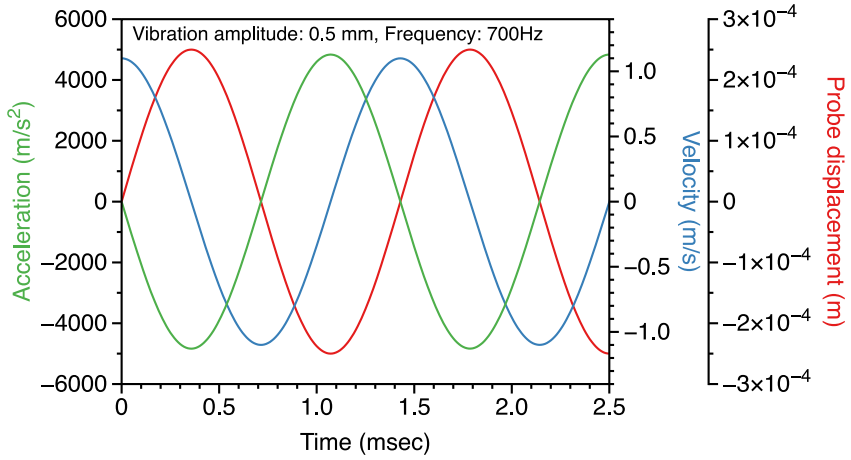

Fig. S15. Time variation of acceleration, speed and displacement of the probe tip.

The time to stretch and break the liquid bridge at the probe end was estimated. We have previously measured the breaking time of liquid bridges using stationary probes[4]. Using aqueous solutions of methanol, ethanol, and 2-propanol, we varied the distance between the probe tip and the glass substrate coated with Rhodamine B and measured the formation and breaking time of the liquid bridges during a single contact and retraction. The results showed that the breaking time of the liquid bridge was directly correlated with the surface tension of the solvent (Fig. S16). In this study, the stretching distance of the

liquid bridge (Table S8) was estimated from the breaking time of the liquid bridge and the speed of the probe[4].

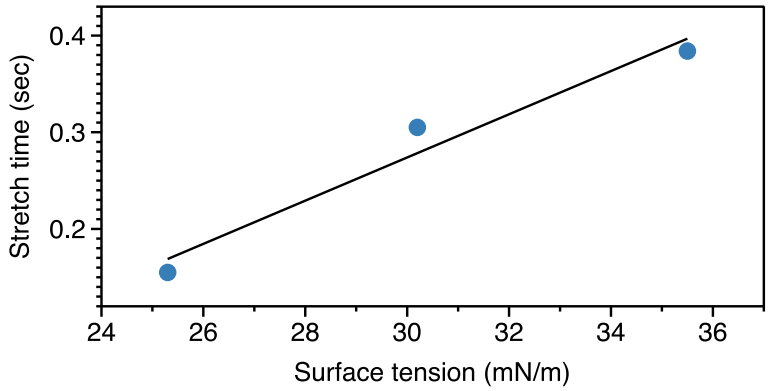

Fig. S16. Relationship between the surface tension and the stretching time of the liquid bridge.

Table S8. The stretch time of the liquid bridge and the probe-sample distance.

Solvent (60 % of alcohol, 0.1% formic acid)	Surface tension (mN/m)	Viscosity (mPa·sec)	Stretch time (sec)	Stretch distance (μm)
MeOH/Water	35.5	1.62	0.384	58
EtOH/Water	30.2	2.52	0.305	47
PrOH/Water	25.3	3.7	0.155	24

The surface tensions of DMF, the mixed solvent and MeOH are 36.2, 29.8 and 23.3 mN/m, respectively. These values are close to the surface tensions of aqueous MeOH, aqueous ethanol, and aqueous 2-propanol, respectively; thus, the stretch distances of these solvents were used for approximation. The maximum speed of the probe tip was estimated from the displacement of the probe tip corresponding to the stretch distance.

References

1 L. Paseta, G. Potier, S. Abbott and J. Coronas, *Org. Biomol. Chem.*, 2015, **13**, 1724–1731.

2 S. Zhang, C. Campagne and F. Salaün, *Appl. Sci.*, 2019, **9**, 402.

3 D. Nakamura, M. Hirano and R. Ohta, *Chem. Commun.*, 2017, **53**, 4096–4099.

4 B. Kamihoriuchi, Y. Otsuka, A. Takeuchi, F. Iwata and T. Matsumoto, *Mass Spectrom.*, 2019, **7**, S0078–S0078.